New coherent Doppler Lidar engine integrating optical transceiver with FPGA signal processor

Toshiyuki Ando(a), Eisuke Haraguchi(a) and Hitomi Ono(a)
(a) Mitsubishi Electric Corporation, Information Technology R&D Center,
5-1-1 Ofuna, Kamakura, Kanagawa, Japan, 247-8501
Ando.Toshiyuki@ap.MitsubishiElectric.co.jp

Abstract: A new coherent Doppler lidar engine has been developed for wind sensing. This new sub-system is consist of a compact optical transceiver board stacking on a FPGA based signal processor board which has small foot print of 26 x 10cm. In the optical transceiver board a pulsed serrodyning transmitter combined with a heterodyning receiver using commercial off the shelf components of the digital coherent optical communication. In the signal processor board, a system on chip embedded processors and a FPGA is used for not only controlling the optical transceiver but also executing lidar data processing without any external host computer, leading to realization of an ultra-compact wind sensing system. Preliminary experiments of line of sight wind velocities with this new lidar sub-system also presented for demonstration.

Keywords: Coherent Doppler LIDAR, Serrodyne Modulation, pulsed modulation

1. Introduction

A Coherent Doppler LIDAR (CDL) is an attractive sensor for wind sensing because it offers a method of remote wind speed measurement in clear atmospheric condition. All-fiber CDL using the wavelength of 1.5 micron has such many advantages as its eye-safety, its reliability for various environmental conditions and its flexibility for deployments [1]. Mitsubishi Electric released 1st generation commercial all-fiber CDL system in 2006[2], [3], and 2nd generation CDL, 'DIABREZZA™ compact' for wind resource assessment in 2014[4]. While the CDL deployments at a steep mountain, small islands, or disaster areas, it needed not only transportable but also battery drivable. The mobile CDL proto type has also demonstrated two-hour successive operation without exchanging batteries [5]. This CDL, however, was not enough small to be transported by one person. This paper presents a new sub-system for realizing a ultra-compact CDL.

2. Introduction

Figure 1 shows a schematic block diagram and outer view of the new coherent Doppler Lidar engine. This new sub-system is consisting of an optical transceiver board which is connected with a signal processing board via FMC connector. The optical transceiver is combined a conventional fiber-optic heterodyning receiver with a newly developed coherent optical pulse seeder based on pulse-serrodyning modulation which is described later in detail. In the signal processing board a system-on-a-chip (SoC) solutions have been adopted by using a large Field Programmable Gate Array (FPGA) with an internal processor core. Measured wind data can be displayed on a tablet PC via the WiFi after on-board signal processing for wind speed estimation. The foot prints of both boards are 26 x 10 cm, the weight is less than 600 g. The designed power consumption is less than 35VA. The power input is a single voltage of DC +12V which can be supplied with commercially available batteries. Both boards are designed with RoHS compliant optical and electrical components taking into consideration of electro-magnetic compatibility (EMC).

Note that this new coherent Doppler Lidar engine can be connected to various types of optical high power amplifiers (OHPA) via the optical fiber connecter, leading to a power-scalable design in system configurations.

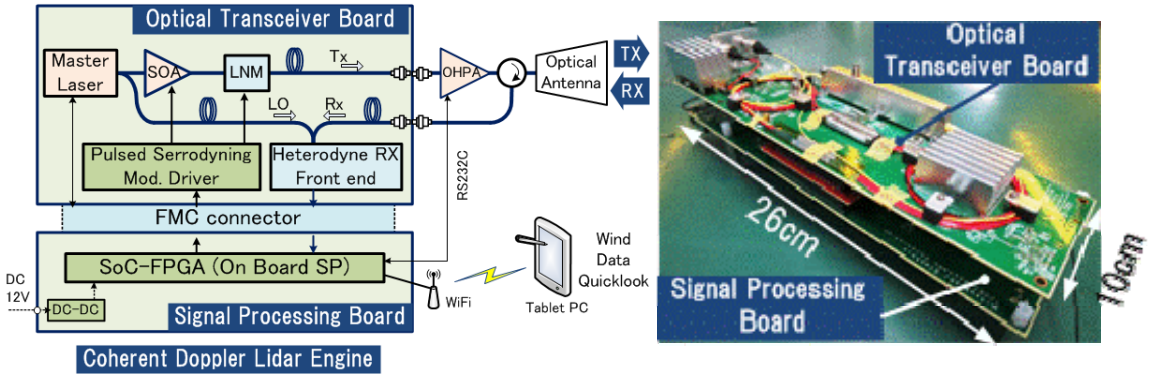

Figure 1. Schematic block diagram and outer view of the new coherent Doppler Lidar engine.

3. OPTICAL TRANSCEIVER UNIT

Figure 2 shows the block diagram and outer view of the optical transceiver unit as a coherent pulse seeder combined with a heterodyne receiver. All fiber-optic components are commercial off the shelf components in the optical communication which have enough high reliability with Telcodia GR468-core compliant. A Distributed Feed Back Laser Diode (DFB-LD) was used as a master laser with line width of 200 kHz and wavelength of 1550 nm. Then its output was split into a local oscillator (LO) and a seed light to a pulsed serrodyning modulator which is consisting of a semiconductor optical amplifier (SOA), a lithium niobate optical phase modulator (LNM) and their drivers with digital-to analog converters (DAC). The pulsed serrodyning modulation is our newly developed technique to realize both pulse modulation and frequency shift without a double-pass AO (Acousto optic) modulator currently used in our CDL system [3].

In a receiver section optical return signals (RX) are phonically mixed with a LO signal, then detected as intermediate frequency (IF) signals at balanced two photo diodes (PD). In order to accommodate a bandwidth of 100MHz corresponding to a range of Doppler frequency of +/- 35m/s, the heterodyning signal is sampled at rate of 216MSps with analog-to digital converter (ADC) and transferred to the signal processing board.

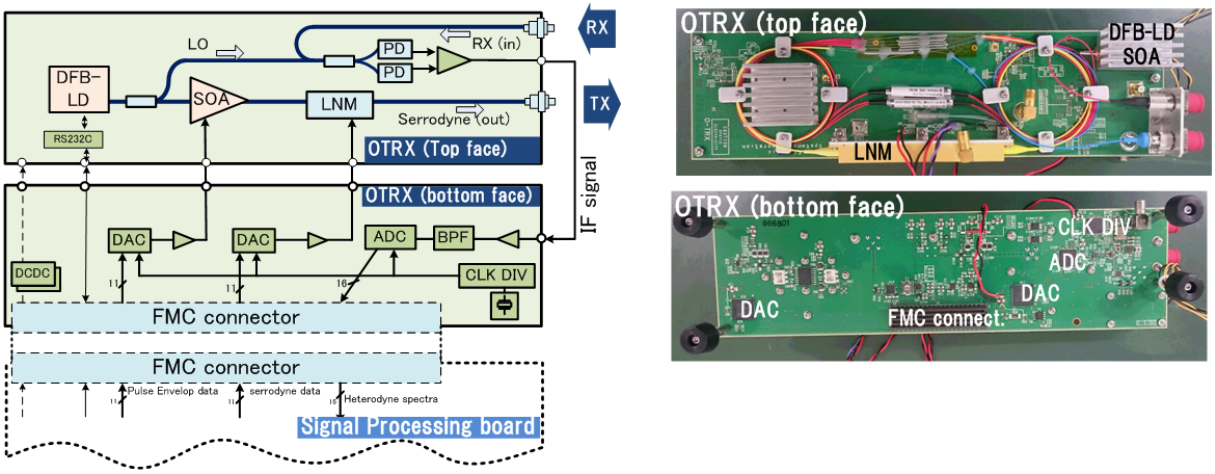

Figure 2. Schematic block diagram and outer view of the optical transceiver unit.

4. PULSED SERRODYNING MODULATOR

Serrodyine frequency shifting is realized by applying a saw-tooth phase modulation to the optical signals, which was originally used for the fiber optic gyroscope with its frequency shift up to several megahertz [6],[7]. Recently frequency shift of a few hundred megahertz as required in CDL can be obtained with a good quality by technological advances in high speed driver electronics. While, SOA is the promising to optical pulse modulator with small foot print if the issue s of frequency chirp is solved [8]. We have newly developed a pulsed serrodyning modulation which realizes both frequency shift and compensation of frequency chirp in SOA.

Figure 3 shows the temporal signals of pulsed serrodyning modulation for an optical intensity of a SOA and an optical phase of a LNM. The saw-tooth phase modulation is applied within only the pulse-on period, T1 over pulse repetition interval (PRI). If the complete saw-tooth phase modulation with cycle of Tm is applied, the output optical frequency is shifted with an offset frequency of 1/Tm.

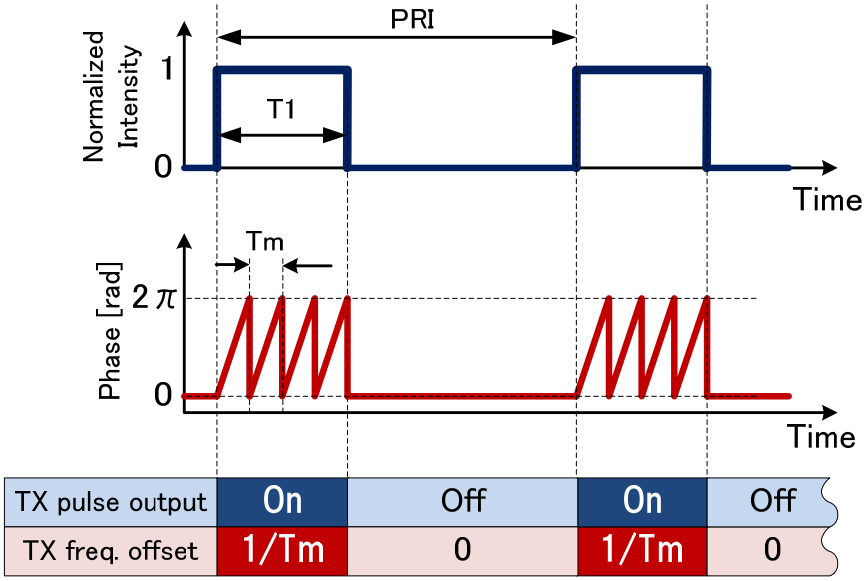

Figure 3. Temporal signals of pulsed serrodyning modulation for an optical intensity of a SOA and a optical phase of a LNM.

It is worthy to note that no frequency shift is occurred within pulse-off periods because of not applying the saw-tooth signal. This leads effective rejection performance of unwanted beat noise between optically internal reflections within pulse-off periods and the LO signal in the heterodyne receiver without such a special pulsed modulator as a double-pass AOM with a high extinction ratio. The technique for compensation of the frequency chirp in a SOA is described in the other paper of this conference [9].

5. SOC-FPGA SIGNAL PROCESSOR UNIT

Figure 4 shows the schematic diagrams and outer view of signal processor unit. In the programmable logic of the SoC-FPGA for receiver section, 256-point fast Fourier transforms (FFT) and incoherent integrations are executed with respect to 80-ranges, stored in buffer memory as raw data of Doppler spectra. In its transmitter section pulsed-serrodyning data are transfer to the DAC on the OTRX board. The processing system of the SoC-FPGA performs post processing of CDL such as subtraction of noise floor in each Doppler spectrum, estimation of wind speed. Calculated wind data are transferred through a GbE interface, which can easily connect to an external tablet PC via the WiFi. This processor can also control external components such as an OHPA, a scanner and a telescope via interfaces of RS-232C and USB.

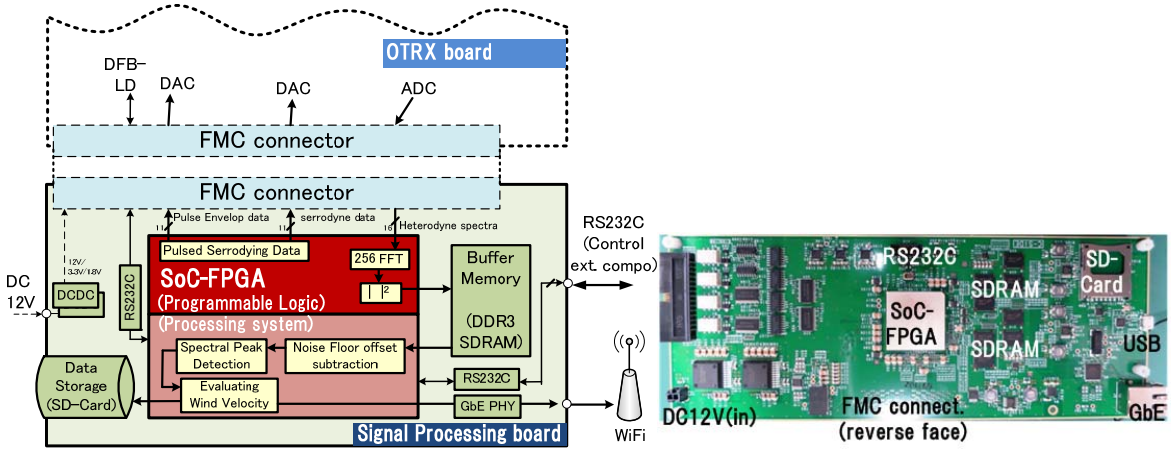

Figure 4. Schematic block diagram and outer view of the signal processor unit.

6. EXPERIMENTAL RESULTS

In order to confirm whether the pulsed-serrodyning modulation does correctly perform, line of sight (LOS) wind Doppler spectra have been evaluated in the case of pulsed-serrodyne modulation and that of single-pass AO modulation as a reference. The measuring condition as follows: the pulse-on period, T1 of 500ns corresponding to range resolution of 75m, a PRI of 250μs, the saw-tooth cycle, Tm of 6.17 ns corresponding to IF of 162MHz as shown in fig.3. Figure 5 (a) shows the LOS wind Doppler spectra at distance of 500m. In the case of single-path AO modulation the spectrum has a strong peak around zero Doppler velocity which may be caused by beat noise between a LO signal and internally reflection of leaky lights within pulse-off periods. This unwanted beat noise makes it difficult to measure wind signals near the zero-Doppler velocity. Meanwhile, the spectrum of pulsed-serrodyne modulation has a peak around -1m/s without any noise peak at zero-Doppler velocity. Figure 5 (b) shows the measurement data of the LOS wind velocity with respect to distance and that of their detectability. Theoretical calculation for detectability is also shown as a function of distance. The setting parameters are as follows: the optical peak power of 20W at a fiber end of an OHPA, the aperture diameter of 50mm, the focusing distance of 500m and the integration number of 4000. The back scattered coefficient is assumed of 8.3e-8 m-1sr-1 taking into account of measured number of aerosol using a particle counter. The measured detectability has considerably agreed with theoretical curve, which indicated the LOS wind velocities are measured up to 900m because of larger detectability than the detection limit of 7dB.

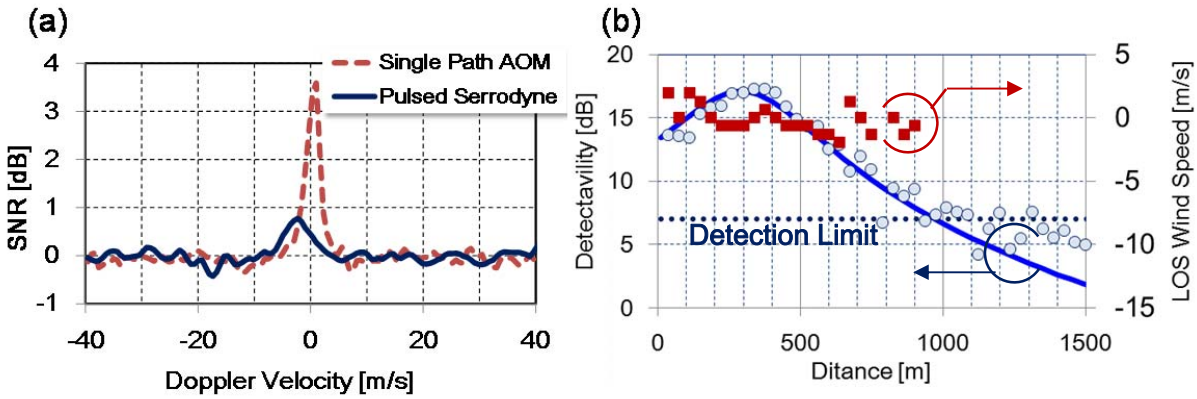

Figure 5. (a) LOS wind Doppler spectra at distance of 500m, (b) LOS wind velocity and detectability with respect to distance

7. SUMMARY

We have developed a new coherent Doppler lidar engine for wind sensing with a small foot print of 26 x 10cm. The pulsed-serrodyning modulation makes it possible to realize both frequency shift and compensation of frequency chirp within pulse-on period of the SOA as pulse modulator. The SoC-FPGA processor performed not only generating saw-tooth signal for pulsed serrodyne modulation but also estimation of wind velocity in RX section including post processing of Doppler spectra. Preliminary experiment of LOS wind velocities demonstrate this new CDL sub-system has been correctly performed.

8. References

[1] S. Kameyama et al, Applied Optics, vol.46, 1953 (2007).
[2] T. Ando et al, 13th Proc. Of Coherent Laser Radar Conference, 170 (2005).
[3] T. Ando et al, IOP Conference Series: Earth and Environmental Science, 1, 012011 (2008).
[4] http://www.mitsubishielectric .co.jp/news/2014/0528.html
[5] T. Ando et al, 17th Proc. Of Coherent Laser Radar Conference (2013).
[6] L.M. Johnson et al, J. Lightwave Technol., vol. 6, 109(1988)
[7] A. Ebbergh et al, Opt. Lett., vol. 10, 300 (1985).
[8] L. Gillner, IEE Proc.-J. Optoelectronics, vol. 139, 331 (1992).
[9] E. Haraguchi et al, 18th Proc. Of Coherent Laser Radar Conference (2016).